Conf-910602--45

EVALUATION OF AGING OF CAST STAINLESS STEEL COMPONENTS*

ANL/CP--70872

DE91 014013

by

H. M. Chung
Materials and Components Technology Division
Argonne National Laboratory
Argonne, Illinois 60439

February 1991

DISCLAIMER

Paper to be presented at ASME Pressure Vessel and Piping Conference, Session on "Nuclear Plant Systems/Components Aging Management and Life Extension," June 23-27, 1991, San Diego, California.

*Work supported by the Office of Nuclear Regulatory Research, U.S. Nuclear Regulatory Commission.

EVALUATION OF AGING OF CAST STAINLESS STEEL COMPONENTS*

H. M. Chung
Materials and Components Technology Division
Argonne National Laboratory
Argonne, Illinois 60439

ABSTRACT

Cast stainless steel is used extensively in nuclear reactors for primary-pressure-boundary components such as primary coolant pipes, elbows, valves, pumps, and safe ends. These components are, however, susceptible to thermal aging embrittlement in light water reactors because of the segregation of Cr atoms from Fe and Ni by spinodal decomposition in ferrite and the precipitation of Cr-rich carbides on ferrite/austenite boundaries. A recent advance in understanding the aging kinetics is presented. Aging kinetics are strongly influenced by the synergistic effects of other metallurgical reactions that occur in parallel with the spinodal decomposition, i.e., clustering of Ni, Mo, and Si solute atoms and the nucleation and growth of G-phase precipitates in the ferrite phase. A number of methods are outlined for estimating aging embrittlement under end-of-life or life-extension conditions, depending on several factors such as degree of permissible conservatism, availability of component archive material, and methods of estimating and verifying the activation energy of aging.

INTRODUCTION

Cast austenitic stainless steels composed of duplex phases of austenite and ferrite are used extensively in the nuclear, oil, and chemical industries because of several superior properties, i.e., higher strength, better weldability, superior resistance to stress corrosion cracking, and soundness of casting (i.e., resistance to hot cracking). In nuclear reactors, cast stainless steels are used heavily for primary-pressure-boundary components that are vital for safe operation of the reactors, e.g., primary cooling pipes, elbows, safe ends, valve bodies, and pump casings. The superior properties of these cast stainless steels are due primarily to the presence of the ferrite phase in the duplex structure. On the other hand, it has long been known that ferritic stainless steels are susceptible to severe embrittlement because of precipitation of the α' phase, a phenomenon commonly termed as "475°C embrittlement". Because of the potential for a similar embrittlement, a series of investigations on thermal aging of cast austenitic stainless steels has been conducted at a number of laboratories, and an extensive data base on mechanisms and kinetics of aging embrittlement of the duplex materials is now available for a large variety of heats aged at temperatures of 280 to 450°C.[1-33] Also, confirmation of thermal aging has been reported for actual field components that were examined after service in BWRs or PWRs.[14,25,26]

Because realistic aging of a component for end-of-life or life-extension conditions at 280–340°C cannot be produced, it is customary to simulate the metallurgical structure of a reactor component by accelerated aging at or near 400°C. It is, therefore, important to validate that the mechanisms of aging embrittlement are identical for the accelerated aging and reactor operating conditions. To extrapolate data on mechanical properties from laboratory to reactor operating conditions, it is also important to understand the kinetics of the metallurgical processes of aging and, more specifically, the temperature dependence (commonly termed as "activation energy") of aging, because a relatively small error in the estimation of activation energy could result in a very significant over- or underestimation of component toughness. Information obtained at a number of laboratories shows, however, that the activation energy of aging embrittlement is strongly influenced by nominally small differences in chemical composition and fabrication process, and a consensus among investigators on the understanding of the activation energy of aging has not been reached yet.

In this paper, further results obtained to provide a better understanding of the behavior of the activation energy of aging are presented with a critical review of various proposed models. The primary purpose of this paper is to present a number of methods of evaluation of end-of-life embrittlement of cast stainless steel components based on an improved understanding of the activation energy of aging.

UNDERSTANDING ACTIVATION ENERGY OF AGING

The aging phenomena of cast stainless steels can be treated on the basis of a simple thermally activated process, according to which kinetics of aging are expressed by an Arrhenius-type equation, i.e.,

$$t_2/t_1 = \exp[Q/R(1/T_2 - 1/T_1)],$$

where t_2 and t_1 are the aging times to reach equivalent material toughness at absolute aging temperatures of T_2 and T_1, respectively, Q is the activation energy of aging, and R is the gas constant. The activation energy of aging, Q, usually defined for aging temperatures between 300 and 400°C, has been based in most investigations on the extent of aging embrittlement measured from room-temperature Charpy-impact tests. Most of the studies of impact properties have shown that the activation energy of aging for the above temperature range is independent of temperature within the limit of uncertainty of measured impact energy, although Bonnet et al.[17] recently reported a trend that the activation energies for a lower temperature range (e.g., 300 to 325°C) are larger than those for a higher temperature range (e.g., 350 to 400°C). This is shown schematically in Fig. 1. Although the temperature-dependent behavior of the activation energy is a real

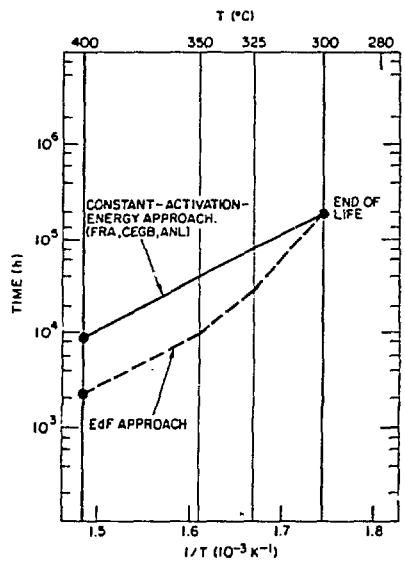

Fig. 1. Schematic Illustration of Selecting Accelerated Aging Conditions Based on Single and Multiple Activation Energies of Aging.

possibility, a further verification appears to be necessary because uncertainty the limit in determining the 300°C impact energies is in general very large and a sufficient number of impact tests must be conducted on specimens that have been long-term aged (i.e., >50,000 h).

Results of earlier investigations of the impact toughness and microhardness of ferritic stainless steels and a number of modified heats of Cu–containing duplex stainless steel showed only high activation energies, close to 210 kJ/mole (50 kcal/mole), a value consistent with an embrittlement mechanism by α' precipitation.[3] Subsequently, however, the extensive data of Trautwein and Gysel[1] on CF–8 and –8M cast stainless steels showed invariably low activation energies in the range of 75-100 kJ/mole (18-24 kcal/mole). This unexpected finding led to an extensive effort among investigators to rationalize the low activation energy. However, no satisfactory explanation could be provided. Results of impact tests, obtained subsequently on a wider variety of CF–3, CF-8, and CF-8M materials, yielded activation energies in the range of 75 to 250 kJ/mole.[4-8] Slama et al.[4] formulated an empirical expression that provides a correlation between the activation energy and bulk chemical composition on the basis of the earlier data reported by Trautwein and Gysel.[1] A similar correlation has been formulated recently[23] from the comprehensive data base of the two investigations[4,23] that produced both high and low values of activation energy. The two empirical correlations, however, do not yield consistent predictions of the aging behavior of some heats.

EARLY MODELS

Models of activation energy of aging proposed in earlier investigations were based on information obtained from tests of mechanical properties alone when definitive evidence of aging mechanisms based on microstructural analyses was not available.

Model Based on Aging Controlled by Interstitial Atoms

In this model, activation energy of aging was assumed to reflect the activation energies of diffusion of interstitial atoms such as C and N in ferrite rather than the metallic atoms of Cr.[3] Although the activation energies of the diffusion of C and N are consistent with the low values of the activation energy of aging in the range of 75-100kJ/mole, this model cannot explain the high activation energies of aging. Even though C or N atoms may play an important role in ferrite embrittlement, the movement of Cr atoms will be a rate-determining process in the precipitation of α' phase or in decomposition by spinodal reaction because diffusivity of Cr atoms is approximately 10^{-8} times slower than that of C or N.[3] The model also implies that the primary mechanism of aging embrittlement is associated with carbide or nitride precipitation in ferrite. This is not consistent with results of subsequent investigations in which spinodal decomposition of ferrite was shown to be the primary mechanism.[15,16,20]

Model Based on Aging by Phase Boundary Precipitation

In this model, aging embrittlement was assumed due to phase- boundary segregation of the interstitial atoms or Cr diffusion on phase boundaries that may lead to phase-boundary precipitation of carbides or nitrides.[3] Although this model is consistent with the low values of activation energy of aging, it is not supported by microstructural evidences. Phase-boundary precipitation of carbides or nitrides has been reported to be only a secondary embrittlement process in certain heats containing high C or N, whereas spinodal decomposition of ferrite phase is the primary embrittlement process of all heats of cast stainless steels aged near or below 400°C.[7,15] Low values of activation energy of aging have been reported for many heats in which phase-boundary precipitation and phase-boundary separation in fractographs were negligible. Also, results from ferrite microhardness measurements are consistent with the low activation energy of aging embrittlement, e.g., for Heats 278 and 280 (Ref. 1 and 13) which indicates that the overall embrittlement is controlled by an in-ferrite process rather than by a phase-boundary process. Also, this model does not explain the long incubation time of aging.[3]

Model Based on Spinodal TTT Curve

It is possible that aging at 400°C is, in some heats of cast stainless steel, near or above the spinodal TTT-curve,[3,7] so that separation of α and Cr-rich α' at 400°C is retarded.[16] According to this model, the dominant mechanism of ferrite embrittlement for aging at 400°C would be nucleation and growth of α' phase rather than spinodal decomposition. However, all the results reported from analyses by field-ion atom-probe (FIAP)[10,11,20] and transmission electron microscopy (TEM)[7,10,22] on specimens of low-activation-energy heats, aged at 400°C, show ferrite decomposition by spinodal reaction rather than by nucleation and growth of α' (e.g., Heat 280 in Ref. 10, Heat 278 in Ref. 11, and Heat A10 in Ref. 20). Therefore, this model seems to be inconsistent with experimental evidence obtained for low-activation-energy heats. Also, this model cannot explain why the low activation energy of aging has not been observed in ferritic alloys.

MODELS BASED ON SYNERGISTIC EFFECTS

Model Based on Clustering and G-Phase Effect on Spinodal Decomposition

It has been proposed that the G-phase precipitation that occurs in parallel with spinodal decomposition in ferrite can influence the rate of the spinodal reaction synergistically, thereby influencing the activation energy of aging.[7] The basis of this model was a premise that unlike the spinodal reaction in an Fe-Cr binary alloy, spinodal decomposition in the ferrite phase of a cast stainless steel involves not only segregation of Fe and Cr but also of Ni. Ni (as well as Mo) solutes were assumed to accelerate the spinodal decomposition near 400°C as they accelerate the "475°C embrittlement" of an Fe-Cr binary alloy.

Precipitation of G phase, which is rich in Ni, Mo, C, and Si, was assumed to deplete the ferrite matrix of Ni and thereby retards the spinodal decomposition relative to a material in which G phase does not precipitate. This effect will be more significant during aging at 400°C than at 300°C because G-phase precipitation is strongly influenced by aging temperature.[7] In a subsequent study, it was shown that activation energies in the range of 75-230 kJ/mole, observed for a large number of heats of CF-3, -8, and -8M grades, could be correlated well with G-phase volume fraction in ferrite after aging at 400°C for 30,000 or 10,000 h (Fig. 2).[14] Later FIAP investigations on Fe-Cr-Ni[24,28] and Fe-Cr-Ni-Mo[28] alloys confirmed the assumption that rates of spinodal decomposition and ferrite hardening are accelerated by both Ni and Mo, an observation that seems to support the model based on G-phase synergism.

Earlier criticisms of this model were based essentially on two aspects: (1) impact energy of a specimen aged at 400°C decreases in general to a saturation level before G-phase precipitates can be observed in significant number density by TEM[16,23] and (2) the extent of Ni depletion from the ferrite matrix via G phase precipitation alone appears insufficient to retard spinodal reaction significantly.[24] Because TEM resolution is limited to a precipitate size larger than ~3 nm, incipient precipitates of G phase or clusters of Ni-Si, Mo-Si, or Ni-Mo-Si (i.e., precursors of G phase) cannot be detected by TEM. Therefore, the exact onset of the clustering and G-phase formation would be difficult to determine by TEM. However, it seems evident that these reactions should occur much earlier in time than indicated by TEM analysis.

In a recent study,[15] early clustering reaction was examined by FIAP on two cast materials in which spinodal reaction was in incipient stage of development. Evaluation of FIAP contingency tables constructed for Ni, Mo, and Si atoms have shown in this study[15] that clustering reactions occur very early, more or less parallel to spinodal decomposition. An example of early profiles of Ni, Mo, and Si, which was obtained by FIAP from a specimen cut from the Shippingport reactor pump volute (Si content 0.96 wt.%, Table 1) are shown in Fig. 3. It can be observed in the figure that Ni-Si and Ni-Mo-Si clusters (denoted by arrows) occur on a fine scale. Result of a similar analysis of the Shippingport hot leg main valve, containing a very low Si level (0.24 wt.%), showed that clustering or G-phase precipitation was absent. In Table 2, a list of evidence obtained from FIAP analysis on the occurrence of Ni-Mo-Si clustering is given. Although results of rigorous analysis were not reported for some of the heats on the basis of contingency tables of Ni, Mo, and Si atoms (as

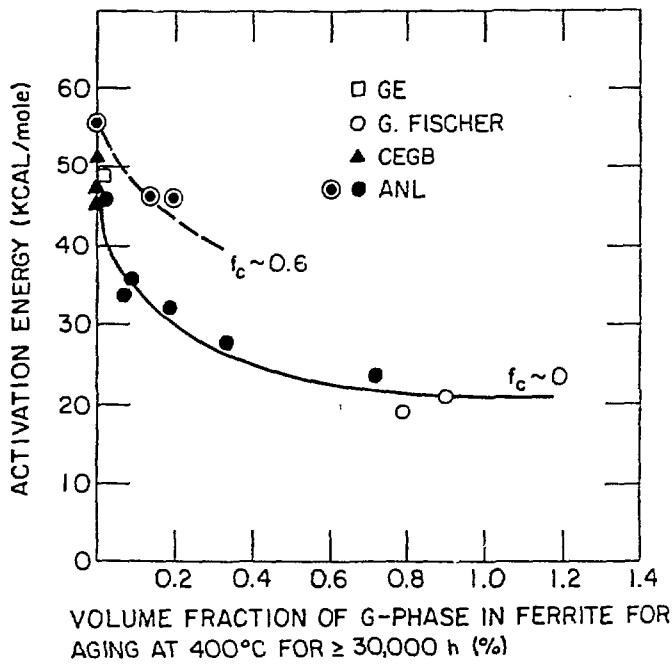

Fig. 2. Activation Energy of Aging versus Volume Fraction of G-Phase in Ferrite Observed after Aging at 400°C for ≥30,000 h. f_c in the figure denotes fraction of the ferrite/austenite boundary covered by $M_{23}C_6$ carbide.

Table 1. Chemical Composition of Reactor Components and Laboratory-Aged Heats Used in This Investigation

Heat No.	Grade	Composition (wt.%) Mn	Si	Mo	Cr	Ni	P	S	N	C	Ferrite Content
KRB BWR Pump Cover[a]											
	CF-8	0.31	1.17	0.17	21.99	8.03	-	-	0.038	0.062	34.0
Shippingport PWR Cold Leg Check Valve[b]											
	CF-8	1.10	1.45	0.01	20.26	8.84	0.018	0.009	0.041	0.056	10.9
Shippingport PWR Hot Leg Main Shut-off Valve[c]											
	CF-8	0.72	0.24	0.24	20.78	10.54	0.041	0.011	0.051	0.052	10.0
Shippingport PWR Pump Volute[d]											
	CF-8	0.50	1.14	0.04	20.79	9.56	0.027	0.017	0.049	0.046	16.2
Ringhals-2 PWR Hot Leg Elbow[e]											
	CF-8M	0.77	1.03	2.09	10.00	10.60	0.022	0.008	0.044	0.037	3.0-22.5
Ringhals-2 PWR Crossover Leg Elbow[f]											
	CF-8M	0.82	1.11	2.08	19.60	10.50	0.020	0.012	0.037	0.039	1.5-15.0
278	CF-8	0.28	1.00	0.13	20.20	8.27	0.008	0.019	0.027	0.038	15.0
280	CF-8	0.50	1.37	0.25	21.60	8.00	0.015	0.006	0.029	0.028	38.0
281	CF-8	0.41	0.45	0.17	23.10	8.60	0.020	0.010	-	0.036	30.0
282	CF-8	0.43	0.35	0.15	22.50	8.53	0.020	0.019	-	0.035	38.0
292	CF-8	0.34	1.57	0.13	21.60	7.52	0.018	0.016	-	0.090	28.0
286	CF-8M	0.40	1.33	2.44	20.20	9.13	0.044	0.015	0.063	0.072	22.0
47	CF-3	0.60	1.06	0.59	18.81	10.63	-	-	0.028	0.018	16.3
51	CF-3	0.63	0.86	0.32	20.13	9.06	-	-	0.058	0.010	18.0
52	CF-3	0.57	0.92	0.35	19.49	9.40	-	-	0.052	0.009	13.5
56	CF-8	0.57	1.05	0.34	19.65	9.28	-	-	0.030	0.066	10.1
59	CF-8	0.60	1.08	0.32	20.33	9.34	-	-	0.045	0.062	13.5
60	CF-8	0.67	0.95	0.31	21.05	8.34	-	-	0.058	0.064	21.1
63	CF-8M	0.61	0.58	2.57	19.37	11.85	-	-	0.031	0.055	10.4
P4	CF-8M	1.07	1.02	2.05	19.64	10.00	-	-	0.151	0.040	10.4
64	CF-8M	0.60	0.63	2.46	20.76	9.40	-	-	0.038	0.038	28.4
65	CF-8M	0.50	0.48	2.57	20.78	9.63	-	-	0.064	0.049	23.4
74	CF-8M	0.54	0.73	2.51	19.11	9.03	-	-	0.048	0.064	18.4
75	CF-8M	0.53	0.67	2.58	20.86	9.12	-	-	0.052	0.065	27.8
Y4331[g]	CF-8M	0.76	1.16	2.59	20.70	10.10	-	-	0.038	0.045	20.0

[a]In service for 8 yr at 284°C in KBR BWR, Gundremmingen, Germany.
[b]In service for 13 yr at 264°C in Shippingport PWR, Shippingport, PA.
[c]In service for 13 yr at 281°C.
[d]Spare pump volute in service only during initial core loading.
[e]In service for 8 yr at 325°C and for 2.5 yr at 303°C in Ringhals-2 PWR, Varberg, Sweden.
[f]In service for 8 yr at 291°C and for 2.5 yr at 274°C.
[g]Contains 0.20 wt.% Nb as impurity.

in Refs. 10 and 15), it seems evident that clustering occurs in an early stage, well before the G- phase precipitate becomes large enough to be detected by TEM.

The clusters are apparently formed more or less homogeneously on a fine scale that is comparable to wavelengths of the spinodal decomposition (Fig. 3). Thus it seems that roles of Ni and Mo in accelerating the spinodal decomposition of ferrite will be suppressed homogeneously as Si atoms trap the Ni and Mo solutes. That is, it appears that this suppression can occur without migration of Ni (and Mo) solutes over a relatively long distance to sinks such as G-phase precipitates. It seems that the clustering reactions in effect reduce a ternary decomposition (involving Fe, Cr, Ni) or quarternary decomposition (involving Fe, Cr, Ni, Mo) to a binary decomposition (involving Fe and Cr only). Assuming that the number of Si and Ni atoms trapped in a Ni-Si cluster is similar, one can estimate that as much as 3-4 at.% (or roughly 3-4 wt.%) of Ni from a total of

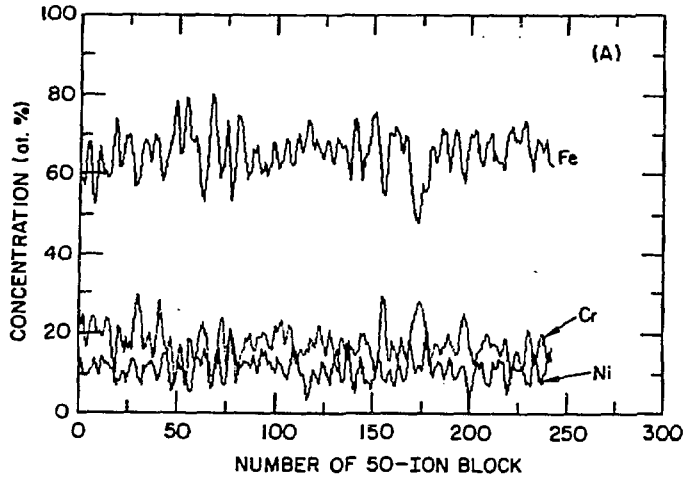

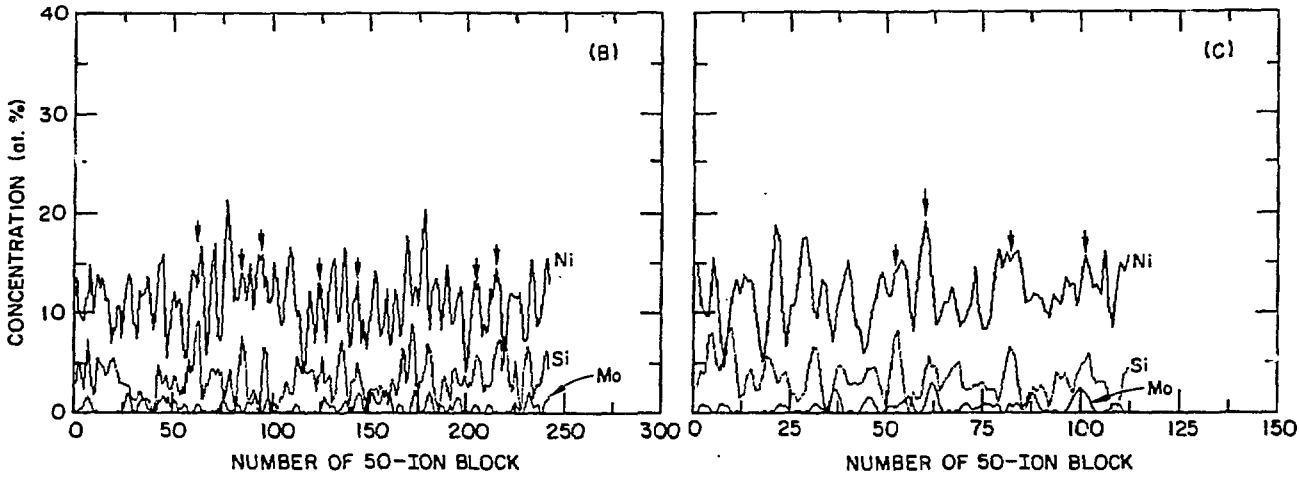

Fig. 3. Results of FIAP Analysis of the Shippingport PWR Pump Volute (Table 1) Showing Spinodal Decomposition and Ni-Si and Ni-Mo-Si Clustering in Ferrite; (A) Fe, Cr, Ni Profiles; (B) Ni, Si, Mo Profiles of (A); and (C) Profiles Similar to (B), Obtained from Another Ferrite Grain of the Same Specimen.

4-6 at.% dissolved in ferrite[13,22] can be trapped by Si, because the Si content in the ferrite of most cast materials is 3-4 at.% (or roughly 1.5 to 2 wt.%; see, e.g., Table 6 in Ref. 15). A similar estimation can be made for Si trapping Mo atoms in a CF-8M material, in which Mo-Si and Ni-Mo-Si clusters are also formed. Therefore, it seems that when Ni-Si, Mo-Si, and Ni-Mo-Si clustering reactions occur in ferrite, a sufficient number of Ni and Mo atoms (i.e., solutes known to accelerate hardening by spinodal decomposition) are likely to be trapped. As a consequence, the rate of spinodal decomposition is retarded significantly relative to a situation in which clustering reactions do not occur. This relative retardation will be more pronounced for aging at 400°C than at 300°C. Consequently, the activation energy of aging will be low. This is illustrated schematically in Fig. 4. Pronounced clustering at 400°C will also result in a significant precipitation of G phase if the material is aged sufficiently long-term (e.g., for 10,000 or 30,000 h, Fig. 2) at that temperature.

A key factor of this model is the relative difference in magnitude of the synergistic interaction for aging at 400 and 300°C. If clusters have already been developed to an advanced stage in a given material even before the start of aging, as in the case of the Shippingport pump volute (Fig. 3), the relative difference will be negligible during subsequent aging at 400 and 300°C. As a result, the activation energy of aging of such material will not be low even though significant precipitation of G phase will be observed (when aged long-term at 400°C). Instead, a relatively high activation energy of aging is expected for such a material, namely, a value comparable to the activation energy of diffusion of Cr in ferrite.

Table 2. Summary of Results of FIAP Analysis of Clustering in Ferrite Phase of Aged Cast Stainless Steel

Heat	Grade	Bulk Composition (wt.%) Ni	Si	Mo	Aging Conditions Location[a]	Temp. (°C)	Time (h)	Evidence of Clustering Between	G-Phase Observed by TEM	FIAP Data Reference
Y3296	CF-8M	10.20	1.21	2.65	FRA	400	8,000	Ni-Si Ni-Mo-Si	Yes	29
Y4331	CF-8M	10.05	1.17	2.58	FRA	400	700	Ni-Si Mo-Si Ni-Mo-Si	No	29
RB3	CF-3	8.70	0.70	0.20	CEGB	300-400	1,000 5,000	None	No	9
A10	CF-8M	10.00	1.22	2.56	EdF	350 350	1,000 2,500	Ni-Si Ni-Si Ni-Mo-Si	No No	20
Main Valve[b]	CF-8	10.54	0.24	0.24	Shippingport Reactor[b]	-	22-yr service	None	No	15
Pump Volute[b]	CF-8	9.56	1.14	0.04	Shippingport Reactor[b]	-	(b)	Ni-Si Mo-Si Ni-Mo-Si	No	15
280	CF-8	8.00	1.37	0.25	GF	300	70,000	Mo-Si	No	10
Fe-25Cr-6Ni-3Mo[c]		6.00	0.72	3.22	Hitachi	450	100	Ni-Si Ni-Mo-Si	No	28

[a]FRA: Framatome, France.
GF: Georg Fischer Co., Switzerland.
CEGB: Central Electricity Generation Board, UK.
EdF: Electricité de France, France.
Hitachi: Hitachi, Ltd., Japan.
[b]See Table 1.
[c]Two-phase alloy, see Ref. 28.

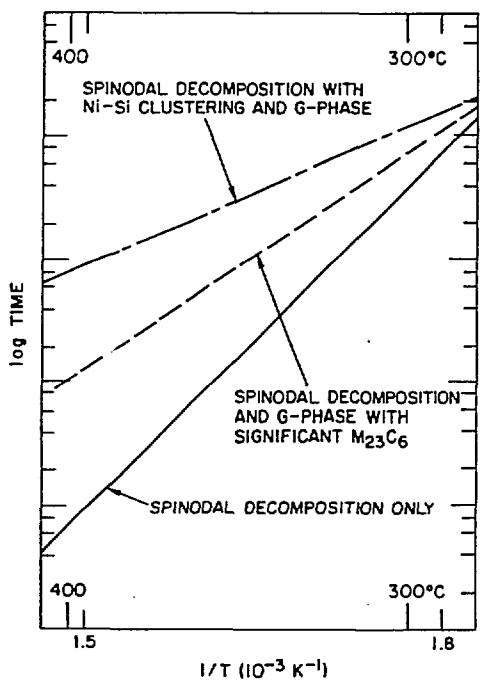

Fig. 4. Schematic Diagram of Relative Kinetics to Produce a Constant-Impact-Energy Drop for Three Hypothetical Cases of Metallurgical Transformation under Otherwise Identical Conditions. (A) Spinodal decomposition only (in ferrite), (B) Ni-Si clustering followed by G-phase precipitation plus (A), (C) significant $M_{23}C_6$ precipitation on austenite/ferrite boundary during aging plus (B).

Model Based on G-Phase Effect on Twinning at 300°C

An alternative model has been also proposed[23] to explain the observed dependence of activation energy of aging on G phase precipitation (Fig. 2). The model is based on an assumption that G-phase precipitation produces a transition of deformation and fracture mechanism (e.g., twinning) of ferrite. According to this model, effects of G phase on aging kinetics at 400°C would be negligible because embrittlement by spinodal decomposition occurs before significant precipitation of G phase. As discussed above, this premise does not take account of formation of G-phase precursors (i.e., clustering reactions) and incipient G-phase precipitates that are not resolved by TEM. For aging at 300°C, the spinodal decomposition and G-phase precipitation occur more or less on the same time scale. Thus, if G-phase precipitation is significant at 300°C, a significant depletion of Ni from ferrite matrix is expected. As a result, twinning in the Ni-depleted ferrite would be suppressed significantly. The result is a relatively faster embrittlement for G-phase-rich specimens aged at 300°C. For specimens aged at 400°C, G phase is unrelated to deformation mode, and twinning is significant for both high- and low-activation-energy heats. Thus, a low activation energy is produced essentially as a result of G-phase-induced suppression of twinning for specimens aged at 300°C.

According to this model, a low-activation-energy heat would be characterized by profuse twinning in 400°C aging and by negligible twinning in 300°C aging. Activation energy of aging would be independent of G-phase behavior at 400°C but strongly dependent on G-phase precipitation at 300°C. However, this seems opposite of the observation shown in Fig. 2. Also, a low-activation-energy heat is generally associated with a relatively slower rate of embrittlement at 400°C (compared to a high-activation-energy heat), rather than with a faster embrittlement at 300°C.[3] This is also inconsistent with the model. As pointed out in Ref. 24, because this model predicts a more pronounced synergism of G phase for a lower aging temperature, it would imply an activation energy that decreases with a lower aging temperature. This is also contrary to the finding reported in Ref. 17 (see Fig. 1). For aging at 300°C, both Ni-Si clustering and G-phase precipitation were negligible in ferrite of low-activation-energy heats[7,10] (for example Heats 278 and 280, aged up to 70,000 h). Therefore, any significant effect of G phase on twinning in specimens aged at 300°C is unlikely, even if twinning is assumed to be a major deformation mode for these specimens.

Model Based on Clustering Effect on Twinning at 400°C

In this model, it is assumed that Ni-Si, Mo-Si, and Ni-Mo-Si clustering reactions in 400°C aging do not influence rate of spinodal decomposition but promotes twinning in ferrite and thereby retard embrittlement in 400°C aging. A similar effect in 300°C aging is assumed to be negligible. This model seems to be consistent with Figs. 2 and 4 but inconsistent with the observation that twinning in ferrite is generally associated with higher Ni content. To determine twinning characteristics in specimens of low-activation-energy heats aged at 400°C, a metallographic examination was conducted in the vicinity of fracture surfaces of room-temperature Charpy-impact specimens of Heats 278, 280, and 286. All three heats have been reported to exhibit low activation energies of aging, ranging from 80 to 100 kJ/mole[1] and a propensity for G-phase precipitation.[14] Specimens aged close to the times of mid-level impact-energy drop (e.g., 3,000 h at 400°C and 70,000 h at 300°C for Heats 278 and 280, and 1,000 h at 400°C and 10,000 h at 300°C for Heat 286) were chosen for examination.

To reveal twins, the specimens were electrolytically etched in a 5% oxalic solution; results are given in Fig. 5. Twins were absent or negligible in all the examined specimens aged at 300°C in the laboratory. Twins were also absent or negligible in the Ringhals-2 PWR elbow specimens that were removed after 10.5 y of service (Table 1). It seems that twinning is not an important deformation mode in specimens aged near 300°C. Only in specimens of Heats 278 and 280, aged at 400°C for 3,000 h, were significant amounts of twins observed near fracture surfaces (Figs. 5A and 5D). However, twins were negligible in specimens of Heat 286 (a similar low-activation-energy heat), aged either at 400°C for 1,000 and 10,000 h, or at 300°C for 10,000 h (Figs. 5G - 5I). These observations therefore indicate that twinning characteristics are not consistent with the activation energy of aging. Nor was the relative propensity of twinning consistent with the characteristics of G-phase precipitation.

Model Based on Austenite Effect on Spinodal Decomposition

In a recent study reported by Brown et al.,[24] the authors measured overall material hardness (using a 30-kg load, compared to the 25-50 gr- load usually used to measure microhardness of ferrite in a duplex

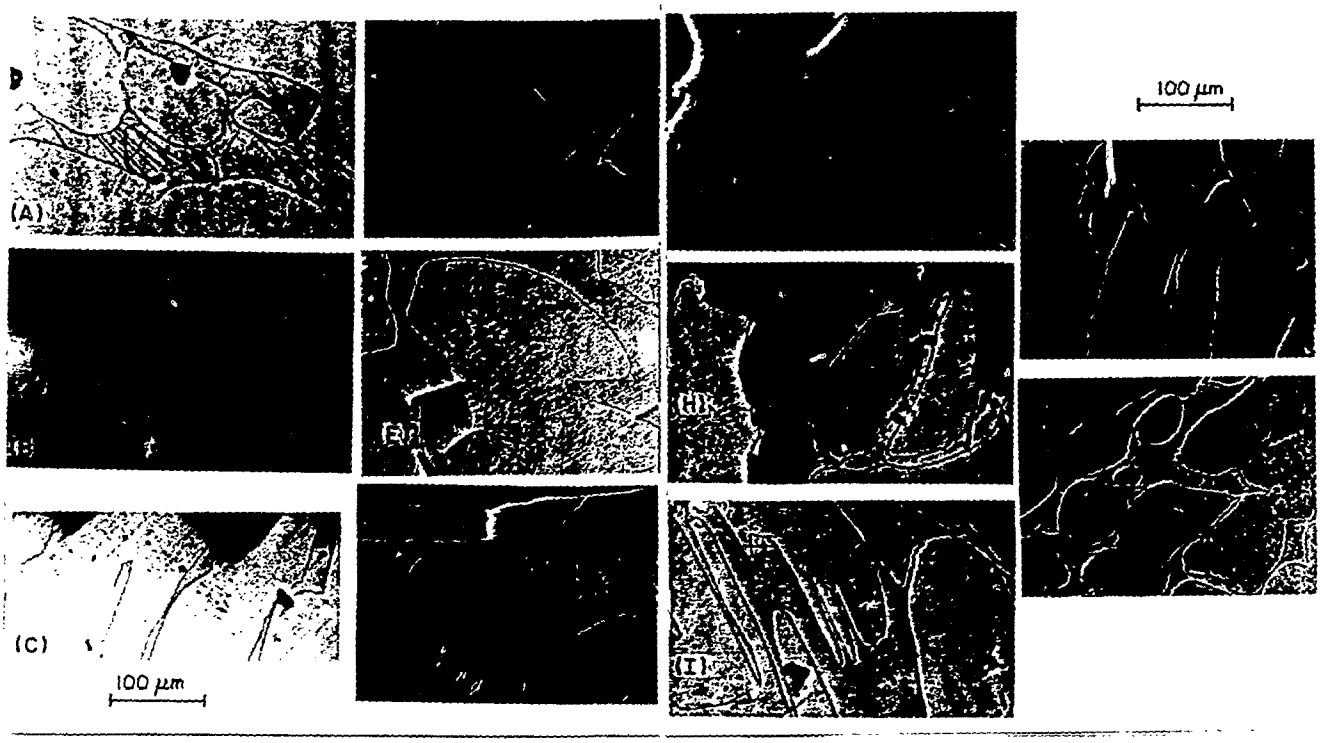

Fig. 5. Metallographs Obtained from Polished and Etched Sections near Room-Temperature Impact-Fracture Surfaces of Specimens of Some Laboratory-Aged Low-Activation-Energy Heats and Ringhals-2 PWR Hot- and Crossover-Leg Elbows (Table 1). (A) - (C) Heat 278 aged, respectively, at 400°C for 3,000 and 10,000 h, and at 300°C for 70,000 h; (D) - (F) Heat 280 aged, respectively, at 400°C for 3,000 h, 350°C for 10,000 h, and 300°C for 70,000 h; (G) - (I) Heat 286 aged, respectively, at 400°C for 1,000 and 10,000 h, and at 300°C for 10,000 h; (J) and (K) Ringhals-2 PWR hot- and crossover-leg elbows, respectively. Twins are denoted with arrows in (A), (B), (D) and (J), and cracks are visible in (C), (E), (H), and (J) across embrittled ferrite.

material) of Fe-26Cr-5Ni alloys after two different thermal treatments that produced, respectively, single ferritic phase and duplex phase. The latter material, containing a minor amount of austenite phase, showed a higher hardness than the former before and after aging. This is probably due to regions of austenite scattered in the material, a situation similar to the increased hardening as a result of γ_2 (small islands of austenite) precipitation in ferrite.[3,7] The relative hardening rates of the single- and two-phase materials of the Fe-26Cr-5Ni, however, appear similar. In view of this, it seems inconclusive if the hardening rate of ferrite in the duplex material was indeed faster than that of the single-phase material. Spinodal amplitudes of the two-phase Fe-26Cr-5Ni and single-phase Fe-28Cr-8Ni specimens, both aged at 450°C rather than 400°C, were also compared. Although the uncertainty limit associated with spinodal-amplitude measurement by FIAP is relatively large, it was reasoned on the basis of the comparison that hardening of ferrite by spinodal decomposition is in general accelerated by the presence of austenite. It was proposed that this behavior may be attributed to an element, more soluble in austenite than in ferrite, that would in effect retard spinodal reaction in single-phase ferrite but that is available in smaller amounts in the ferrite phase of a duplex material.[24] However, it is not clear how this premise can explain the low activation energy of aging, since the effect of austenite will be similar for both aging at 300 and 400°C. Ni is generally partitioned preferentially in austenite than in ferrite.[15] However, less Ni in ferrite of a duplex material than in a single-phase ferritic material will result in a faster spinodal reaction in the latter than in the former; this is opposite of the premise. It has been generally known that low activation energies of aging have been reported only for duplex materials and that single-phase ferritic materials always show a high activation energy. As pointed out earlier[3] and confirmed recently,[27] a low activation energy of aging of a duplex stainless steel

tends to be associated with a slower rate of aging at 400°C relative to a ferritic material. That is, it is not associated with a slower rate of aging at 300°C. This is consistent with the model illustrated in Fig. 4 but inconsistent with the premise that hardening of ferrite by spinodal decomposition is accelerated by the presence of austenite in a duplex material.

METHODS OF EVALUATING END-OF-LIFE AGING

A number of different methods can be used to evaluate the aging degradation of a given components for an end-of-life or life-extension situation. The specific method to be chosen will depend on several factors, i.e., degree of permissible conservatism, availability of archive or an equivalent material, method of estimating activation energy of aging, and type of mechanical testing of the acceleration-aged specimens. An implicit but important assumption made in the evaluation is that thermal aging is the only significant degradation mechanism for a given component.

Method A

In this method, only the minimum saturated impact energy and a corresponding fracture toughness value are estimated for conservative evaluation of aging. Therefore, no information on kinetics or activation energy of aging is required. Minimum (room-temperature) impact energy corresponding to the saturated state of aging is known to be sensitive to ferrite content, ferrite spacing, and chemical compositions and can be expressed by either of the following two equations:[27]

$$\log_{10}C_{Vsat} = 1.15 + A\exp(-BF), \qquad (1)$$

where

C_{Vsat} = minimum room-temperature saturation impact energy (C_V in J/cm^2),
A = 1.374 for CF-3 and -8, and 1.532 for CF-8M,
B = 0.0365 for CF-3 and -8, and 0.0467 for CF-8M,
$F = f_c\,(Cr+Si)(C+0.4N)$ for CF-3 and -8, and
$f_c\,Cr(C+0.4N)(Ni+Si)^2/100$ for CF-8M, and
f_c = ferrite content (in %).

$$\log_{10}C_{Vsat} = 1.386 + 0.938\exp(-0.0205F) \qquad (2)$$

where

$F = f_c\,(Cr+Mo+Si)(C+0.4N)NiL/10^4$, and
L = mean ferrite spacing (in μm).

In these equations, ferrite content can be either measured or calculated from bulk chemical compositions. However, the mean ferrite spacing must be measured on an available piece of archive material or on an actual component.

Apparently, ferrite content (f_c) is the predominant factor that influences the minimum saturated impact energy. For example, Bonnet et al.[17] showed that saturated minimum impact energies of 62 laboratory-aged heats reported in Refs. 1, 4, and 17 can be correlated well with measured ferrite contents only. This seems to be because ferrite content itself is related to chemical composition. The simple correlation, shown by Bonnet et al., also gave an equally good approximation of the minimum impact energies that were reported from this laboratory on CF-8 and CF-8M heats[23,30] and recovery-annealed-and-reaged reactor components,[26] with the exception of CF-3 heats[23,30] (e.g., Heats 47, 51, and 69). This is shown in Fig. 6. Impact energies of the three CF-3 heats were somewhat higher than those predicted on the basis of ferrite content. The simple correlation between the minimum saturated impact energy and ferrite content can be expressed by the equation:

$$\log_{10}C_{Vsat} = 2.40 - 0.0385\,f_c, \qquad (3)$$

where C_{Vsat} and f_c are in J/cm^2 and %, respectively. Because Eq. (3) underpredicts actual minimum impact energies for CF-3 heats, it seems that the simple correlation can be used to estimate conservatively saturated impact energies for all cast steels regardless of grade, heat, and chemical composition.

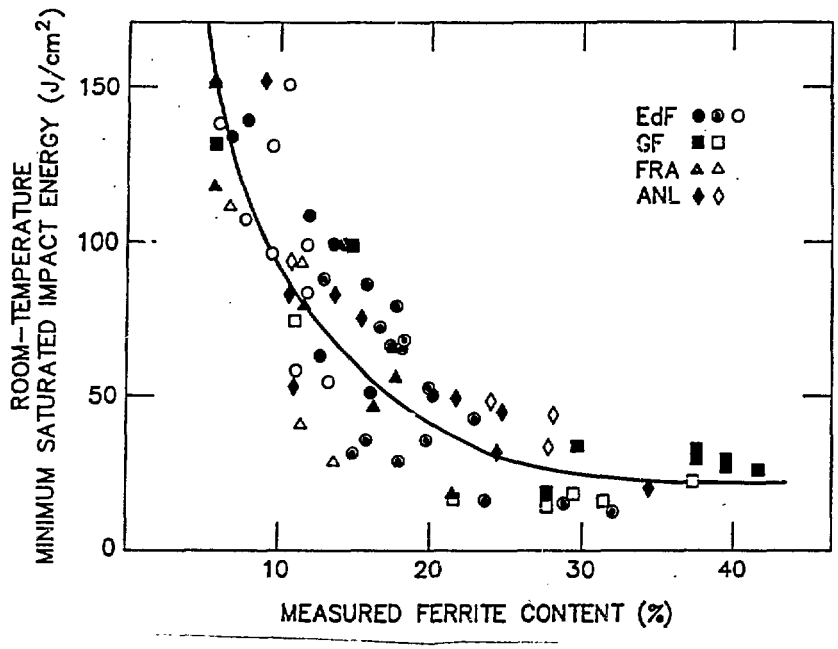

Fig. 6. Room-Temperatrue Saturated Impact Energy vs. Measured Ferrite Content Plotted for Heats Reported in Refs. 1 (GF), 4 (FRA), 17 (EdF), 26 (ANL), and 30 (ANL).

Ferrite content can be calculated to a satisfactory accuracy from either of the following two equations (from Refs. 17 and 27, respectively):

$$f_c \text{ (in \%)} = (21.8R^2 - 5.96R + 3.39)[400/(1500 - T)], \quad (4)$$

where

$R = (Cr + Mo + 0.65Si - 17.6)/(Ni + 20C + 8.3N + 0.08Mn - 5.18)$, and

T = temperature of final solution heat treatment (in °C).

$$f_c = 100.3(Cr_{eq}/Ni_{eq})^2 - 170.72\ (Cr_{eq}/Ni_{eq}) + 74.22, \quad (5)$$

where

$Cr_{eq} = Cr + 1.21Mo + 0.48Si - 4.99$, and

$Ni_{eq} = Ni + 0.11Mn - 0.0086(Mn)^2 + 18.4N + 24.4C + 2.77$.

These equations have been reported to predict ferrite contents within an accuracy of 3 and 6%, respectively, of measured values.

Fracture toughness can be derived from the relationship:[27]

$$J_d = A\ (C_V)^n\ (a_c)^m, \quad (6)$$

where J_d = deformation J (in kJ/m^2),

C_V = room-temperature impact energy (in J/cm^2) and,

a_c = crack extension (in mm).

For room-temperature fracture toughness, the constants A, n, and m for CF-3 and -8 are, respectively, 37.5, 0.52, and 0.60, and for CF-8M, they are 8.2, 0.85, and 0.50, respectively. Similar values of A, n, and m for fracture toughness at 290-320°C are, respectively, 48.5, 0.45, and 0.45 for CF-3 and -8, and 34.3, 0.52, and 0.45 for CF-8M grade. Use of this method corresponds to a significant degree of conservatism but does not require availability of an archive material.

Method B

This method incorporates kinetics of aging to reduce the degree of conservatism. Evaluation is made as described below to give a more realistic estimation of aging for given temperature and lifetime. However, an accelerated aging test on an archive or an equivalent material is required.

1. Determine activation energy of aging based on the empirical correlation:[23]

$$Q(kJ/mole) = 90.54 + 9.62Cr - 8.12Ni - 7.53Mo + 20.59Si - 123.0Mn + 317.7N, \quad (7)$$

where chemical compositions are given in wt.%.

2. Determine time for accelerated aging at 400°C based on the estimated activation energy of aging and end-of-life or life-extension time- at-temperature, e.g., as in Fig. 1.
3. Conduct the accelerated aging at 400°C for the determined time on a Charpy-impact or fracture toughness specimen.
4. Measure room-temperature impact energy and derive fracture toughness according to Eq. (6), or conduct a J-R curve test to measure fracture toughness directly, or both.

Method C

An activation energy determined from Method C will always be subject to uncertainties associated with the validity limit of the empirical correlation given by Eq. (6). This concern has been raised primarily in association with the data reported by Trautwein and Gysel.[1] Activation energy based on the data of Trautwein and Gysel has been predicted from a separate correlation developed by Slama et al.:[4]

$$Q(kJ/mole) = -66.65 + 6.90Cr - 5.44Ni + 8.08Mo + 17.15Si + 44.1Mn + 297.1N. \quad (8)$$

For most heats within ASTM Specification A351 and with normal fabrication histories, Eq. (6) appears to give a satisfactory prediction of activation energies. However, this cannot be ensured for every case with a given field component, even if one can show on the basis of chemical composition and heat treatment that Eq. (7) must be used instead of Eq. (8). Activation energies of some heats seem to exhibit a significant deviation from values determined from either Eq. (7) or (8). Some examples are activation energies of aging of some cast stainless steel specimens obtained from decommissioned reactor components, e.g., the KRB BWR pump cover and the Shippingport PWR check and main valves (Table 1). Estimated values for these components based on Eq. (7) are 234, 122, and 126 kJ/mole, respectively (Table 3). However, actual values based on impact energy and reported recently on these components[26] are 168, 170, and 180-226 kJ/mole, respectively. These values correspond to a significant deviation from both Eq. (7) as well as Eq. (8). Deviations of this magnitude are certain to lead to a large error in estimated aging.

The measured activation energies, however, seem to agree fairly well with the values predicted earlier[14] on the basis of microstructural analysis, i.e., 168, 168, and 210 kJ/mole (Table 3). The microstructure-based prediction of the service-aged components was derived from TEM and FIAP analyses of Ni-Mo-Si clustering, G-phase precipitation, and austenite-ferrite boundary carbide precipitation in accordance with the model illustrated in Fig. 4. Although carbide precipitation can be predicted reasonably well on the basis of C and Mo contents, experiences show that Ni-Mo-Si clustering, and hence G-phase precipitation, cannot be predicted by bulk chemical composition (e.g., Si, Ni, and Mo contents). Only in extreme cases, was a reasonable prediction possible, e.g., heats of CF-3 and -8 grades containing very low Si (< 0.3 wt.%) or heats of CF-8M grade containing high Si (> 1.0 wt.%). Clustering and G phase precipitation were negligible in the former but pronounced in the latter.

The complex behavior of clustering and G-phase precipitation, and hence their influence on activation energy, appears to be the primary factor associated with the limitations of the empirical correlations. By proper microstructural techniques, however, one can analyze the characteristics of clustering and precipitation of G phase and carbides, and a fairly accurate value of activation energy can be predicted regardless of grade, heat, chemical composition, and fabrication history.[14] This is demonstrated for the heats given in Table 3. FIAP analysis of early-stage clustering is not an easy task. However, if a specimen is aged

Table 3. Summary of Activation Energy (in kJ/mole, and kcal/mole in parenthesis) Estimated for Some Reactor Components and Laboratory-Aged Heats from Empirical and Microstructure-Based Correlations

Heat or Component[a]	From Eq. (8)	From Eq. (7)	From Microstructure-Based Correlation[b]	Actual Observed[c]
KRB BWR Pump Cover	88 (21)	234 (56)	168 (40)	160 (38)
Shippingport PWR Cold Leg Check Valve	75 (17)	122 (29)	168 (40)	170 (41)
Shippingport PWR Hot Leg Main Valve	59 (14)	126 (30)	210 (50)	180 -226 (43 -54)
Shippingport PWR Pump Volute	80 (19)	190 (45)	210 (50)	202 (48)
278	63 (15)	214 (51)	92 (22)	80 (19)
280	88 (21)	67 (16)	92 (22)	88 (21)
281	83 (20)	210 (50)	–	138 (33)
282	75 (18)	201 (48)	–	201 (48)
286	101 (24)	92 (22)	92 (22)	101 (24)
292	92 (22)	235 (56)	101 (24)	92 (22)
47	67 (16)	147 (35)	130 (31)	138 (33)
56	63 (15)	164 (39)	235 (56)	230 (55)
59	67 (16)	172 (41)	180 (43)	197 (47)
63	80 (19)	109 (26)	92 (22)	101 (24)
P4	83 (20)	122 (29)	113 (27)	117 (28)

(a) See Table 1 for chemical compositions.
(b) From Ref. 14.
(c) Determined from room-temperature impact energies reported in Refs. 1, 26, and 27.

at 400°C for 10,000 h or longer, clustering can be deduced from TEM without conducting the more cumbersome FIAP analysis.[14] The procedure in this methods would then be:

1. Age the archive or equivalent material at 400°C at several aging times (e.g., 300, 1,000, 3,000, 10,000 h) and obtain a complete curve of impact energy (or J_d) vs. aging time.

2. Conduct TEM (and FIAP, if possible) analysis to determine the extent of G-phase and carbide precipitation, and from these results estimate the corresponding activation energy of aging according to the method given in Ref. 14.

3. Determine the aging time at 400°C that is equivalent to end of life from the estimated activation energy and obtain equivalent impact and fracture-toughness values.

Method D

If the kinetics of accelerated aging can be determined (namely, a complete curve of impact-energy vs. time for aging at 400°C), the activation energy of aging can be estimated from an empirical correlation that is based on chemical composition and the measured kinetics for aging at 400°C:[27]

$$Q(\text{kJ/mole}) = 10\,[74.06 - (7.66 - 0.46\,I_1)\,s - 4.35\,Si + 1.38\,I_2\,Mo - 1.67\,Cr - (2.22 + 3.56\,I_1)\,Mn + (108.8 - 75.3\,I_1)\,N], \quad (9)$$

where $I_1 = 0$ and $I_2 = 1$ for CF-3 or CF-8, and $I_1 = 1$ and $I_2 = 0$ for CF-8M, and s = logarithm of time of aging at 400°C to reach mid-level impact energy, i.e., the average of the two impact energies that correspond to unaged and saturated aging conditions. Once the activation energy is estimated, material toughness can be obtained as in Method C.

Method E

Methods B, C, and D can be used in a complementary manner to determine a more accurate value of activation energy and to minimize the number of tests required. For example, determine the accelerated aging time at 400°C based on Eq. (7), and conduct aging and microstructural analyses on a specimen aged for that time. If the activation energies of aging estimated from the two methods are similar, then determine J_d as in Method B. If agreement is poor, conduct analyses as in Methods C and D.

METHODS OF AGING DIAGNOSIS

In addition to prediction of aging degradation for an end-of-life or life-extension condition, it would be very useful to have the capability of measuring and verifying the severity of aging for a given component at a given time of service. Although the practical applicability of nondestructive evaluation of aging on field components does not appear promising, several diagnostic techniques are being developed. These techniques are based essentially on detection of changes in various physical and electrochemical properties that are produced as a result of Cr-rich alpha-prime formation in ferrite phase. Because ferrite contents can be determined reasonably accurately from Eqs. (3) or (4) or from actual measurement, a measurement of aging of the ferrite phase can provide a reasonable diagnosis of overall component degradation, although exact values of impact or fracture toughness cannot be obtained.

If small metallographic specimens can be obtained from the inside and outside surfaces of a component, diagnosis of aging can be conducted by several techniques. A measurement of ferrite microhardness or spinodal amplitude provides information on extent of aging of ferrite.[15,24] Diagnostic methods have been also investigated on the basis of measurements of magnetic properties[31,32] and electrochemical potentiokinetic ratio. However, these studies have been conducted primarily on specimens aged at 450°C or higher. In this temperature range, ferrite hardening is produced by nucleation and growth of spherical α' precipitates, a phase containing Cr up to 80 wt.%. However, ferrite structure is produced during aging under reactor service conditions via spinodal decomposition and is believed to be a sponge-like structure in which the maximum local content of Cr is no more than 45 wt.%. Therefore, signals of magnetic or electrochemical potentiokinetic properties are expected to be relatively small. Further investigation in this area seems necessary, including a demonstration of the techniques on field components and development of methods to calibrate the obtained signals.

CONCLUSIONS

1. Analysis of mechanical properties and microstructural characteristics obtained on a large number of heats of CF-3, -8, and -8M grades shows that an approach based on accelerated aging at 400°C can be used to evaluate aging for service at 280-340°C. In this approach, the most important factor influencing the accuracy of the evaluation is the activation energy of aging, i.e., the temperature dependence of aging kinetics of a given component. Aging kinetics are strongly dependent on chemical composition, ferrite content, and thermomechanical history during fabrication. The rates of the metallurgical processes associated with the aging embrittlement (i.e., spinodal decomposition of ferrite, Ni-Mo-Si clustering and G-phase precipitation in ferrite, and precipitation of carbides in ferrite and on ferrite-austenite

boundaries) are strongly influenced by these variables. Kinetics of spinodal decomposition (i.e., the primary mechanism of aging) are in particular strongly influenced by nominally small differences in fabrication process and ferrite chemical composition, notably that of Ni, Mo, Si, and C. Decomposition rate also appears to be influenced strongly by Ni–Si, Mo-Si, and Ni-Mo-Si clustering that occurs in tandem with the spinodal reaction before G-phase precipitation.

2. A critical review of several models proposed to explain the complex behavior of activation energy of aging has been given. No model appears to provide a satisfactory explanation except that based on the synergism between the spinodal decomposition and Ni-Si, Mo-Si, and Ni-Mo-Si clustering, which are precursors of G-phase precipitation.

3. Several methods have been outlined that can be used to evaluate aging for end-of-life or life-extension conditions. Selection of a specific method depends on several factors such as degree of permissible conservatism, availability of archive or equivalent material, use of accelerated aging, and methods of estimation and verification of the activation energy of aging.

ACKNOWLEDGMENTS

This work was supported by the Office of Nuclear Regulatory Research, U.S. Nuclear Regulatory Commission. Thanks are due to A. Trautwein of G. Fischer Co., Switzerland and C. Jansson of Vattenfall Energisystem, Sweden, for kindly making available the laboratory- and reactor-aged specimens for analyses of microstructure and twinning behavior.

REFERENCES

1. A. Trautwein and W. Gysel, Spectrum, Technische Mitteilungen aus dem GF Konzern, May 1981, 5; also in Stainless Steel Castings, (eds. V. G. Behal and A. S. Melilli), 165; 1982, ASTM STM 756, Philadelphia, ASTM.

2. E. I. Landerman and W. H. Bamford, Am. Soc. Mech. Eng., MPC–8, 99 (1978).

3. H. D. Solomon and T. M. Devine, Jr., "Duplex Stainless Steels -- A Tale of Two Phases," Report No. 82CRD276, General Electric Co., Nov. 1982.

4. G. Slama, P. Petrequin, and T. Mager, Presented at SMiRT Post–Conference Seminar 6, Assuring Structural Integrity of Steel Reactor Pressure Boundary Components, Aug. 29–30, 1983, Monterey, CA.

5. K. N. Akhurst and P. Pumphrey, "The Aging Kinetics of CF–3 Cast Stainless Steel in the Temperature Range 300°C to 400°C," Report RD/L/3354/R88, Central Electricity Generating Board Research Laboratories, United Kingdom, Nov. 1988.

6. Y. Meyzaud, P. Ould, P. Balladon, M. Bethmont, and P. Soulat, Proc. Intl. Conf. on Thermal Reactor Safety (NUCSAFE 88), Oct. 2–7, 1988, Avignon, France.

7. H. M. Chung and O. K. Chopra, in Proc. 3rd Intl. Symp. on Environmental Degradation of Materials in Nuclear Power Systems --Water Reactors, (eds. G. J. Theus, and J. R. Weeks), pp. 359–370; 1988, Warrendale, PA, The Metallurgical Society.

8. O. K. Chopra and H. M. Chung, ibid., pp. 737–748.

9. M. K. Miller and J. Bentley, ibid., 341-349.

10. J. M. Sassen, M. G. Hetherington, T. J. Godfrey, G. D. W. Smith, P. H. Pumphrey, and K. N. Akhurst, Report MPC–Vol. 26, ASME PVP–Vol. 132, Properties of Stainless Steels in Elevated Temperature Service, American Society of Mechanical Engineers, New York, NY, 65–78, 1987.

11. H. M. Chung and O. K. Chopra, ibid., pp. 17-34.

12. O. K. Chopra and H. M. Chung, ibid. pp. 79-105.

13. T. Godfrey and G. D. W. Smith, Proc. 33rd Field Emission Symp., Berlin, July 7-11, 1986, J. de Physique, Colloque C7, Suppl. No. 11, Vol. 47, Nov. 1986, pp. 217-222.

14. H. M. Chung, Proc. ASME Pressure Vessel and Piping Conference Session on Life Assessment and Life Extension of Power Plant Components, July 23-27, 1989, HI, ASME PVP-Vol. 171, 111-125

15. H. M. Chung and T. R. Leax, Proc. International Workshop on Intermediate Temperature Embrittlement Processes in Duplex Stainless Steels, August 1-2, 1989, Oxford, England, Mat. Sci. Tech. Vol. 6, pp. 249-262 (March 1990)

16. P. H. Pumphrey and K. N. Akhurst, ibid.

17. S. Bonnet, J. Bourgoin, and M. Guttman, ibid.

18. G. E. Hale and S. G. Garwood, ibid.

19. S. G. Druce and M. Strangwood, ibid.

20. P. Auger, F. Danoix, A. Menand, S. Bonnet, J. Bourgoin, and M. Guttman, ibid.

21. T. R. Leax, S. S. Brenner, and J. A. Spitznagel, ibid.

22. H. M. Chung and O. K. Chopra, "Accelerated Aging Embrittlement of Cast Duplex Stainless Steels - Activation Energy for Extrapolation," in Proc. 4th Intl. Symp. Environmental Degradation of Materials in Nuclear Power Systems- Water Reactors, August 6-10, 1989, Jekyll Island, GA, in press.

23. O. K. Chopra, Proc. ASME Pressure Vessel and Piping Conference Session on Degradation of Ferritic, Austenitic, and Duplex Stainless Alloys in Nuclear Service, June 17-21, 1990, Nashville, TN, ASME PVP-Vol. 195, pp. 193-214

24. J. E. Brown, M. G. Heatherington, G. D. W. Smith, and P. H. Pumphrey, ibid.

25. C. Jansson, "Degradation of Cast Stainless Steel Elbows after 15 Years in Service," Proc. Fontevraud II International Symposium, Sept. 10-14, 1990, Fontevraud, France.

26. O. K. Chopra, "Studies of Aged Cast Stainless Steel from the Shippingport Reactor," Proc. 18th Water Reactor Safety Information Meeting, Oct. 22-24, 1990, Rockville, MD.

27. O. K. Chopra, "Estimation of Fracture Toughness of Cast Stainless Steels in LWR Systems," ibid.

28. T. Yoshimura and Y. Ishikawa, "Atom-Probe Characterization of Aged Stainless Steels," paper presented at ASME Annual Meeting, Nov. 25-30, 1990, Dallas, TX.

29. T. R. Leax, Westinghouse Electric Corp., private communication, 1988.

30. O. K. Chopra and H. M. Chung, Proc. 16th Water Reactor Safety Information Meeting, Oct. 24-27, 1988, Gaithersburg, MD, NUREG/CP-097, Vol. 3, pp. 519-545.

31. M. Ohtaka, K. Enomoto, K. Hasegawa, and T. Shimizu, Proc. ASME Pressure Vessel and Piping Conference Session on Nondestructive Evaluation: NDE Planning and Application, July 23-27, 1989, HI, ASME NDE-Vol. 5, pp. 225-230.

32. G. Donaldson, S. Evanson, M. Ohkata, K. Hasegawa, T. Shimizu, and K. Takaku, British J. NDT, 32 (1990), 238-240.

33. C. E. Jaske and V. N. Shah,"Life Assessment Procedures for Major LWR Components," NUREG/CR-5314, EGG-2562, Vol. 3, Idaho National Engineering Laboratory, EG&G Idaho, Inc., October, 1990.